High-order Adaptive Mesh Refinement Multigrid Poisson Solver in any Dimension

Erwan Deriaz

Équipe Modélisation et Contrôle

IRMA, CNRS / Université de Strasbourg

CANUM 2020 – Minisymposium AMR

Évian – 14 Juin 2022

Overview

Poisson solvers in Physics simulation

Poisson Equation in dimension d:

$$\Delta u = v, \quad \text{with} \quad \Delta = \sum_{i=1}^{d} \partial_i^2 \tag{1}$$

Exemple: Reduced MHD

$$\frac{\partial F}{\partial t} + [\varphi\, ,\, F] = \rho_s^2[U\, ,\, \psi] + \eta(\Delta\psi - \Delta\psi_{eq}), \tag{2}$$

$$\frac{\partial U}{\partial t} + [\varphi\, ,\, U] = [\psi\, ,\, \Delta\psi] + \nu(\Delta U - \Delta U_{eq}), \tag{3}$$

$$\left(Id - de^2\Delta\right)\psi = F \qquad \Delta\varphi = U. \tag{4}$$

2D Magnetic Reconnection Simulation

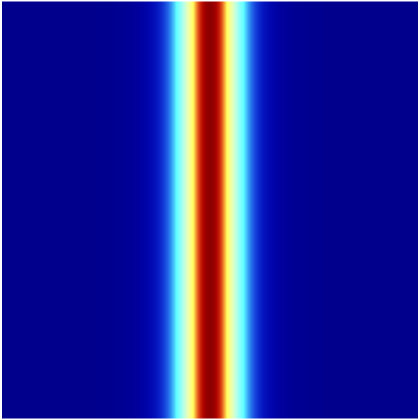

Magnetic stream F

refinement level of the grid

Turbulence

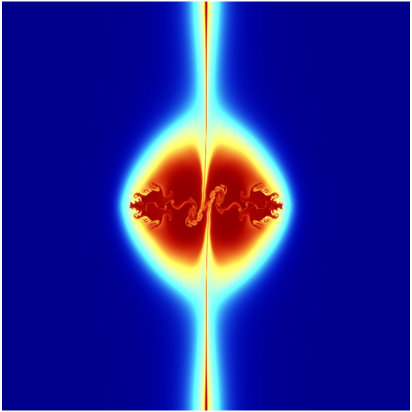

complex structured

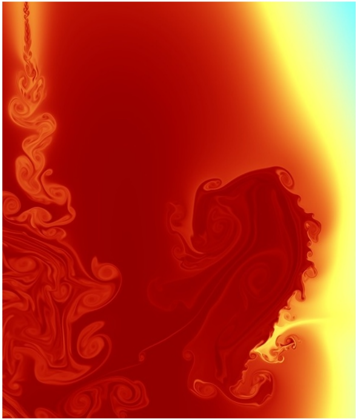

multiscaled turbulence

Poisson Solvers, State-Of-the-Art

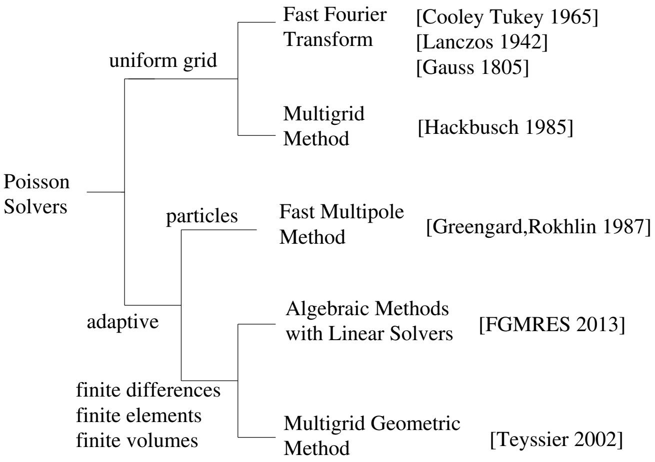

Overview

Adaptive Mesh Refinement Tree structure

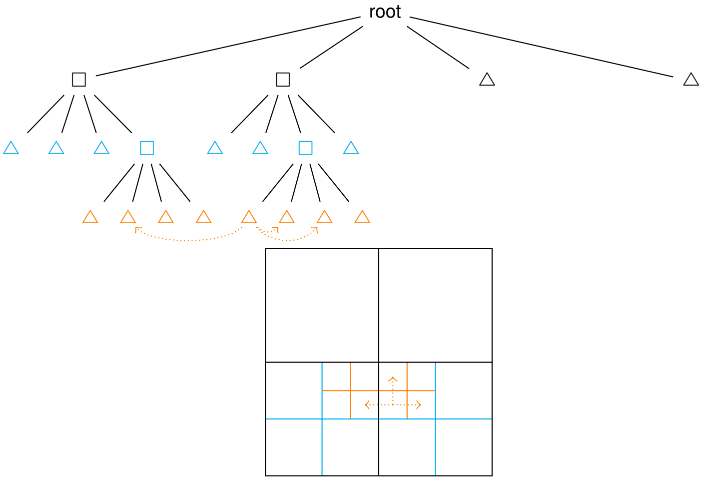

Figure: Fully-threaded tree (top) and its associated non-uniform grid (bottom).

Cell-based/vertex-based

- refinement centered on the cell

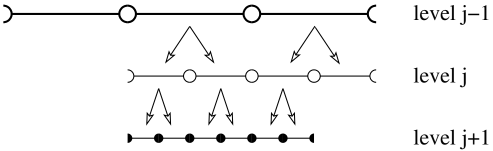

- refinement centered on the point

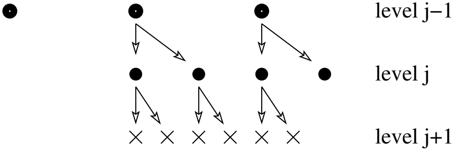

Point activation

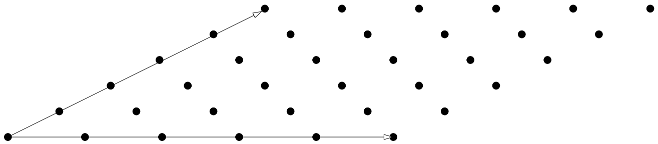

Point activation

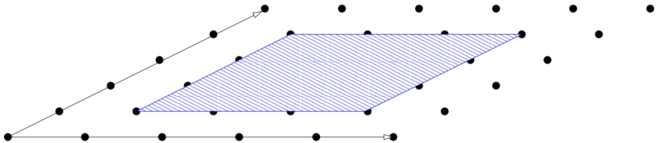

Point activation

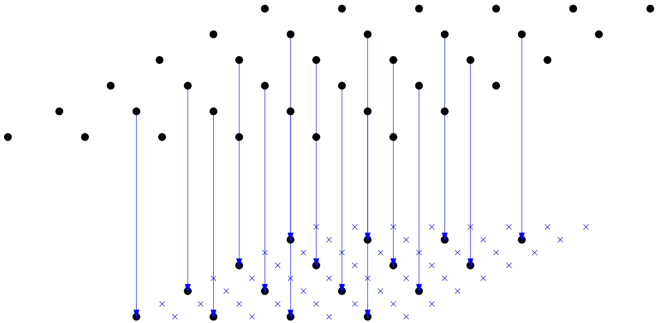

Point activation

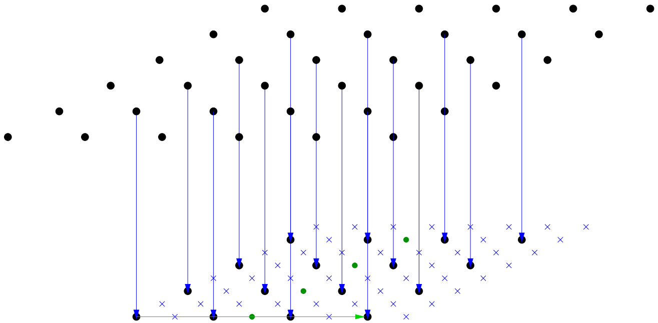

Point activation

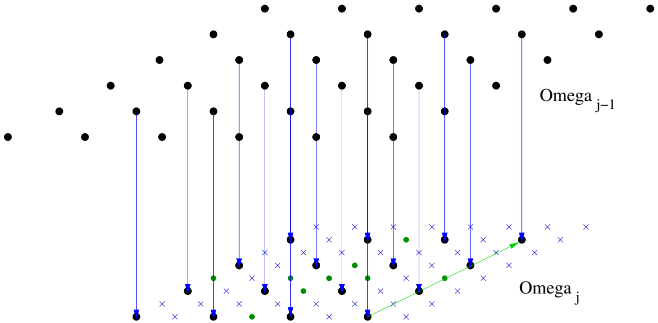

Point activation

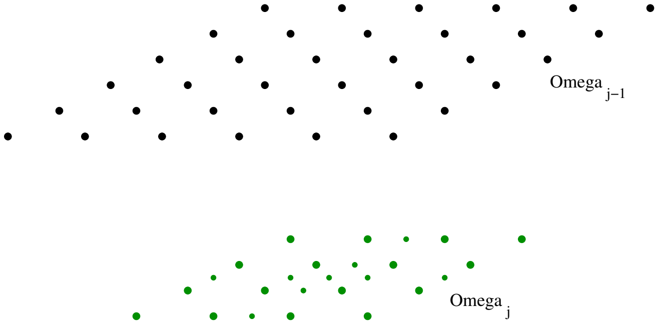

Boundary of a refined subdomain

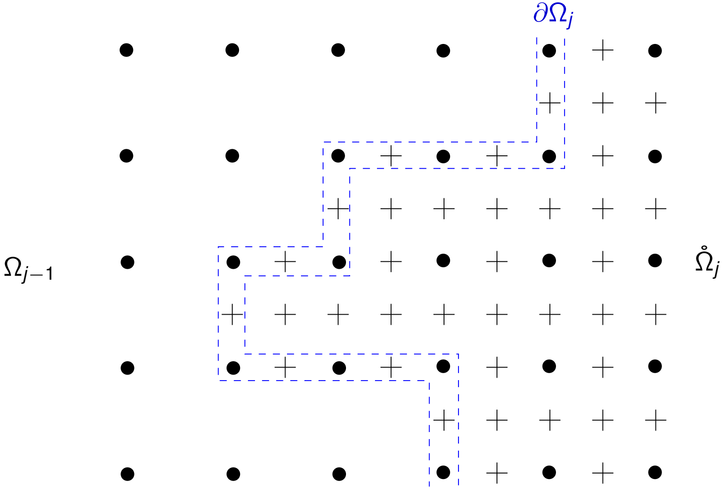

Figure: Example of domain Ω_j divided between its boundary $\partial\Omega_j$ and its interior $\mathring{\Omega}_j$.

Boundaries

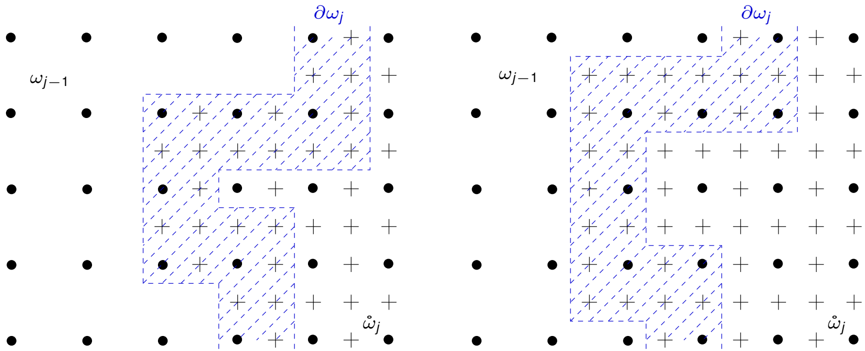

Figure: Two different ways of fixing the boundary.

Overview

2D usual non-compact stencil

$$\frac{1}{12h^2}\begin{matrix} & & -1 & & \\ & & 16 & & \\ -1 & 16 & -60 & 16 & -1 \\ & & 16 & & \\ & & -1 & & \end{matrix}\; u = v \qquad (5)$$

“Mehrstellenverfahren” scheme

$$\frac{1}{6h^2}\begin{bmatrix} 1 & 4 & 1 \\ 4 & -20 & 4 \\ 1 & 4 & 1 \end{bmatrix} u = \frac{1}{12}\begin{bmatrix} & 1 & \\ 1 & 8 & 1 \\ & 1 & \end{bmatrix} v \qquad (6)$$

6th order any-dimensional case

$$A = \alpha[p \;\; 1 \;\; p]^d + \begin{array}{ccccc} & & \gamma & & \\ & & | & & \\ \gamma & - & \beta & - & \gamma \\ & & | & & \\ & & \gamma & & \end{array} \tag{7}$$

namely

$$a_{\mathbf{0}} = \alpha + \beta, \quad a_{(1,0,\ldots,0)} = \alpha\, p + \gamma, \quad \text{and} \quad a_{(\underbrace{1,\ldots,1}_{k \text{ times}},0,\ldots,0)} = \alpha\, p^k \quad \text{for} \quad k \geq 2.$$

To reach the sixth-order accuracy, computations lead to:

$$p = \frac{1}{3}, \quad \alpha = \frac{3}{2}\left(\frac{3}{5}\right)^{d-2}, \quad \beta = -\frac{25+2d}{6} \quad \text{and} \quad \gamma = \frac{1}{6}.$$

6h order any-dimensional case

$$B = \omega [q \;\; 1 \;\; q]^d + \begin{array}{ccccccccc} & & & & b_{01} & & & & \\ & & & & | & & & & \\ & & & & 0 & & & & \\ & & & & | & & & & \\ b_{01} & - & 0 & - & \lambda & - & 0 & - & b_{01} \\ & & & & | & & & & \\ & & & & 0 & & & & \\ & & & & | & & & & \\ & & & & b_{01} & & & & \end{array}$$

namely

$$b_{\mathbf{0}} = \omega + \lambda, \quad b_{(\underbrace{1,\ldots,1}_{k \text{ times}},0,\ldots,0)} = \omega\, q^k \quad \text{for} \quad k \geq 1, \quad \text{and} \quad b_{(2,0,\ldots,0)} = b_{01},$$

with

$$q = \frac{1}{7}, \quad \omega = \frac{9}{10}\left(\frac{7}{9}\right)^d, \quad \lambda = \frac{1}{10} + \frac{d}{120} \quad \text{and} \quad b_{01} = -\frac{1}{240}.$$

10th order 3-dimensional case

Bottom half of the symmetric three-dimensional stencil:

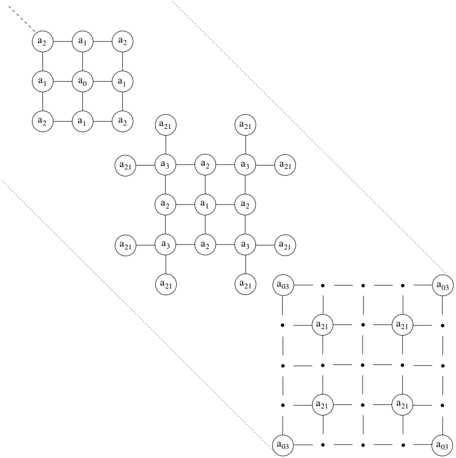

There are 113 points for the B stencil: b_0, b_1, b_2, b_3, b_{01}, b_{11}, b_{02}, b_{03}, b_{001}, b_{101}, b_{0001}.

Overview

In the uniform case, the V–cycle

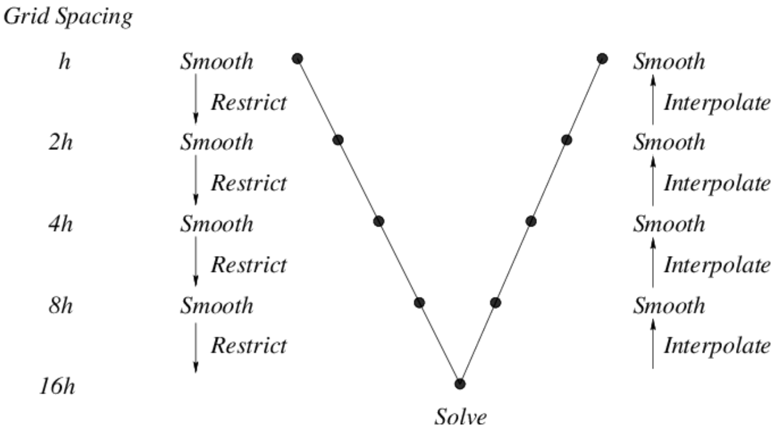

[Colin Fox]

Gauss-Seidel iterations

Gauss-Seidel iteration (Smoother): for $x_\lambda \in \mathring{\omega}_j$ do

$$tmp_{n+1}(x_\lambda) = tmp_n(x_\lambda) + \frac{h^2}{a_{\mathbf{0}}}\left(res(x_\lambda) - \frac{1}{h^2}A\ tmp_n(x_\lambda)\right)$$

Interpolation of the boundary

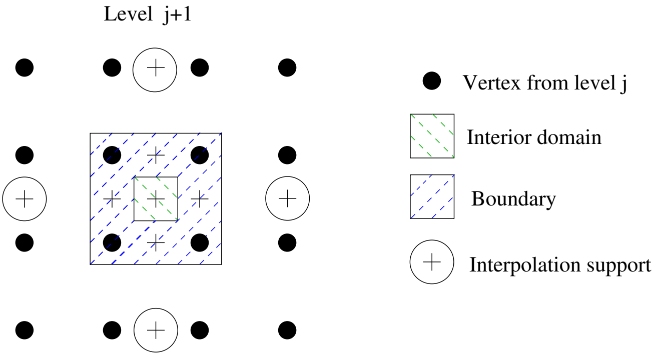

Figure: Instance of fourth-order consistent distribution of vertices with their types. Only one among the horizontal couple of interpolatory points or the vertical one is necessary.

Interpolets

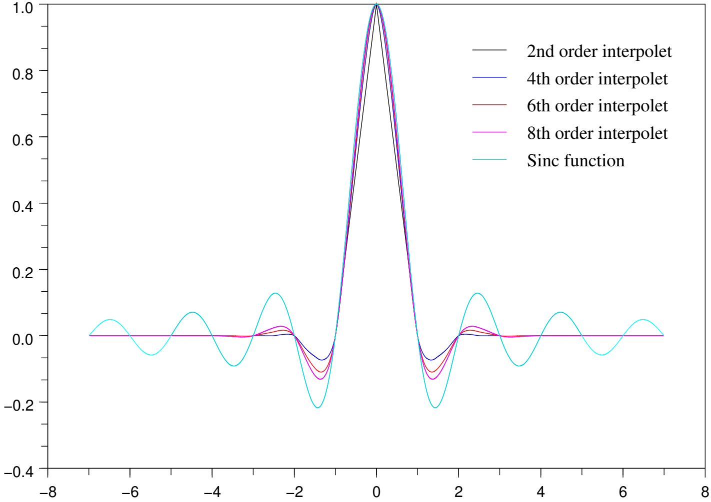

Figure: Interpolets of 2nd, 4th, 6th and 8th orders tending to the sinc function.

Overview

Test case: the Gaussian

$$u(\mathbf{x}) = \exp\left(-\frac{r^2}{\sigma^2}\right) \tag{8}$$

with $r = |\mathbf{x}|$ and the parameter σ small enough.

$$v(\mathbf{x}) = \left(\frac{4|\mathbf{x}|^2}{\sigma^4} - \frac{2d}{\sigma^2}\right)\exp\left(-\frac{|\mathbf{x}|^2}{\sigma^2}\right)$$

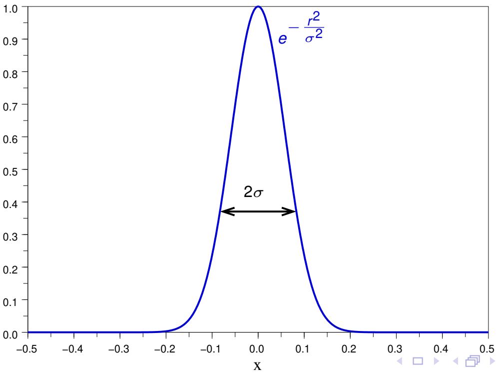

Convergence of the algorithm

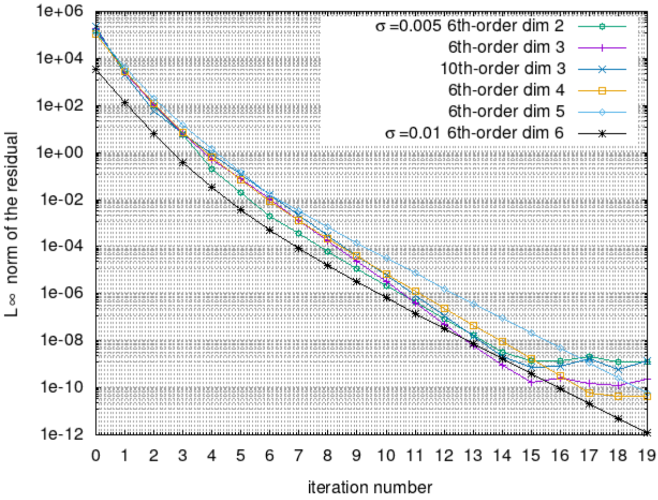

Figure: Convergence process of the multigrid algorithm. The first iterations achieve the largest reductions of the residual.

Accuracy 6th order stencils

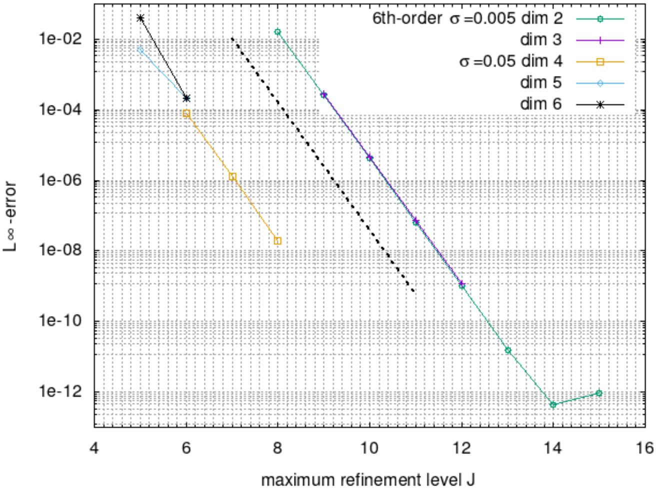

Figure: Order of convergence for the 6th-order scheme in various dimensions. The dashed line represents the 6th-order slope.

Accuracy 10th order stencil

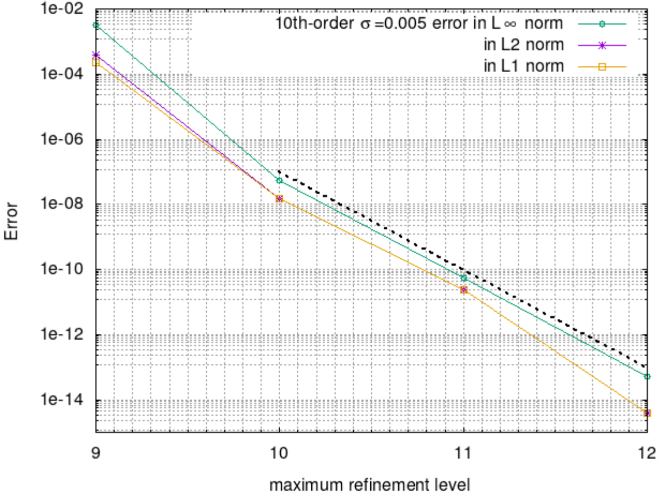

Figure: Convergence for the 3-dimensional 10th-order scheme in various norms. The dashed line represents the 10th-order slope.

Convergence with a continuous refinement

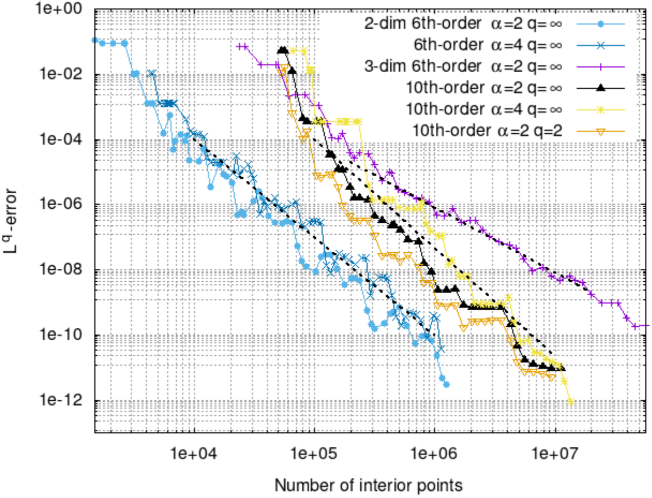

Figure: Experimental L^q-error as a function of the number of points. The theoretical slopes $\varepsilon_{L^q} = KN_{pt}^{-p/d}$ ($\frac{p}{d} = \frac{6}{2}, \frac{10}{3}, \frac{6}{3}$ from left to right) are represented by dashed lines.

Overview

Cost comparison with FMM

Total cost C of the multigrid Poisson solver:

$$C = (\#B + N_{it}(4\#A + 2 \times 3 + 2(2p + 2)))\, N_{pt} \qquad (9)$$

$\#B$ and $\#A$ stand for the numbers of non zero elements of the stencils B and A, N_{it} the number of V-cycle iterations, N_{pt} the number of points and $2p$ the order of the method.
For instance, the 3-dimensional 6th-order HOC stencil verifies $\#A = 27$, $\#B = 25$ and only needs 12 iterations to converge to the computer rounding error so its cost is given by $C = 1585N_{pt}$. Of course it is possible to decrease this cost by fixing a larger error tolerance and taking fewer iterations. For instance converging to 10^{-6} only takes 5 iterations then the cost is given by $C = 675N_{pt}$.

This compares advantageously to the costs given for the pth-order Fast Multipole Method whose optimal implementation in 3 dimensions yields

$$C = 200N_{pt}p + 3.5N_{pt}p^2.$$

Which means $C = 1326N_{pt}$ for the 6th-order $p = 6$ case.

Experimental computational time with OpenMP

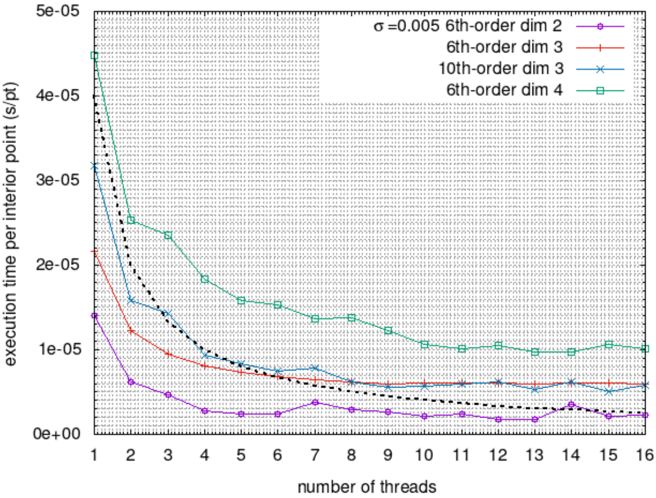

Figure: Time per interior point to converge to $\|\Delta u_n - \Delta u\| < 10^{-10}\|\Delta u\|$ when varying the number of threads.

Overview

Conclusion – Perspectives

Original vertex-centered AMR multigrid Poisson solver of any orders and for any dimensions.

Perspectives:

- direct computation of the gradient of the potential from the density function as it is done in Fast Multipole Methods,
- MPI-parallelization,
- introduction of immersed boundary to provide an AMR immersed boundary scheme